Topical Review

Functional source separation and hand cortical representation for a brain–computer interface feature extraction

Franca Tecchio[1,2], Camillo Porcaro[2], Giulia Barbati[2] and Filippo Zappasodi[1,2]

[1]*Istituto Scienze e Tecnologie della Cognizione - CNR, Rome, Italy*
[2]*AFaR - Centre of Medical Statistics and IT, Fatebenefratelli Hospital, Rome, Italy*

A brain–computer interface (BCI) can be defined as any system that can track the person's intent which is embedded in his/her brain activity and, from it alone, translate the intention into commands of a computer. Among the brain signal monitoring systems best suited for this challenging task, electroencephalography (EEG) and magnetoencephalography (MEG) are the most realistic, since both are non-invasive, EEG is portable and MEG could provide more specific information that could be later exploited also through EEG signals. The first two BCI steps require set up of the appropriate experimental protocol while recording the brain signal and then to extract interesting features from the recorded cerebral activity. To provide information useful in these BCI stages, our aim is to provide an overview of a new procedure we recently developed, named functional source separation (FSS). As it comes from the blind source separation algorithms, it exploits the most valuable information provided by the electrophysiological techniques, i.e. the waveform signal properties, remaining blind to the biophysical nature of the signal sources. FSS returns the single trial source activity, estimates the time course of a neuronal pool along different experimental states on the basis of a specific functional requirement in a specific time period, and uses the simulated annealing as the optimization procedure allowing the exploit of functional constraints non-differentiable. Moreover, a minor section is included, devoted to information acquired by MEG in stroke patients, to guide BCI applications aiming at sustaining motor behaviour in these patients. Relevant BCI features – spatial and time-frequency properties – are in fact altered by a stroke in the regions devoted to hand control. Moreover, a method to investigate the relationship between sensory and motor hand cortical network activities is described, providing information useful to develop BCI feedback control systems. This review provides a description of the FSS technique, a promising tool for the BCI community for online electrophysiological feature extraction, and offers interesting information to develop BCI applications to sustain hand control in stroke patients.

(Resubmitted 26 January 2007; accepted after revision 20 February 2007; first published online 1 March 2007)
Corresponding author F. Tecchio: ISTC – CNR, Unità MEG, Dipartimento di Neuroscienze – Ospedale 'Fatebenefratelli', Isola Tiberina, Rome, Italy. Email: franca.tecchio@istc.cnr.it

A brain computer interface (BCI) can be defined as any system that can track the person's intent which is embedded in his/her brain activity and, from it alone, translate the intention into commands of a computer (Fig. 1). Thus a BCI creates a link between two adaptive systems. One of these systems is the neural network within the brain, generating signals during the processing of individual intention of an action. This network uses sensory evaluation of action outcomes to adapt and optimize these signals. The second system is the computer, reached by the brain signals provided by the monitoring system. The BCI decoding algorithm must adapt to these signals and their adaptation and optimization to implement the translation of intention into action. Since the two systems are linked, neither is truly independent. Among the brain signal monitoring systems best suited for this challenging task, electroencephalography (EEG) has the two properties that are essential for most realistic BCIs: non-invasiveness and portability. Magnetoencephalography (MEG) has the

 DOI: 10.1113/jphysiol.2007.129163

same non-invasiveness as EEG and, although it is not portable, it allows selective focus on specific aspects that could be later exploited by EEG. Invasive BCIs, where the brain signal comes from implanted electrodes (e.g. subdural, epidural or intracortical electrocorticogram, ECoG), are, in fact, at their origin since the suitability of the recorded signal is lost over a few months (Maynard *et al.* 1997; Navarro *et al.* 2005) and the electrodes have to be removed, although long technological strides have been made on implantable electrodes.

The first BCI applications were developed to help people with total loss of any control on voluntary musculature (including respiratory and oculomotor – a situation defined as 'locked in') in communicating with the environment and other people. In addition, applications could be developed to relieve the suffering of extremely diseased people, induced by pathologies leaving unaffected a minimal amount of neuromuscular connections sustaining patients' communication abilities (such as amyotrophic lateral sclerosis in its final stages, cerebrovascular accidents, brain and spinal cord traumas, severe muscular dystrophies, Parkinson's disease, severe forms of multiple sclerosis). Moreover, efforts in developing BCI provide information that is also useful for different applications, including the control of prosthetic limbs (Prochazka *et al.* 1997; Lauer *et al.* 2000*a*; Craelius, 2002; Popovic, 2003) and neuroprostheses (Stein *et al.* 1992; Lauer *et al.* 2000*b*; Popovic & Sinkjaer, 2000), or other hybrib bionic systems (HBSs), like exo-skeletons and tele-operated platforms.

For BCI to be effective in real-world applications, many challenges must be addressed and overcome (Moore, 2003). The required cognitive load must be minimized through optimization of the cerebral activity extraction. In fact, while most BCI systems are tested in quiet laboratory environments, where users are able to concentrate on the task at hand with minimal distractions, BCI users in the real world have to deal with much more complex situations, including emotional responses, interactions with other people, and safety considerations. Every BCI has its own operational protocol which defines the procedures for switching on and off, the continuity or discontinuity of the communication, whether the relevant signal is generated consciously by the subject or in response to a stimulus triggered by the BCI (event-related), the exact sequence of interactions between the subject and the BCI, and the type of feedback provided to the subject. In real life the subject must be able to choose the message and to carry out the switching on and off procedures.

Feature extraction

The feature extraction stage processes the cerebral data and extracts relevant features to feed the translation algorithm (Fig. 1). The cerebral data are acquired by some monitoring system, using appropriate experimental protocol designs. Data are then AD converted, using the sampling rate suitable to the cerebral signal being processed, at least twice the expected highest relevant frequency component in the signal of interest. The

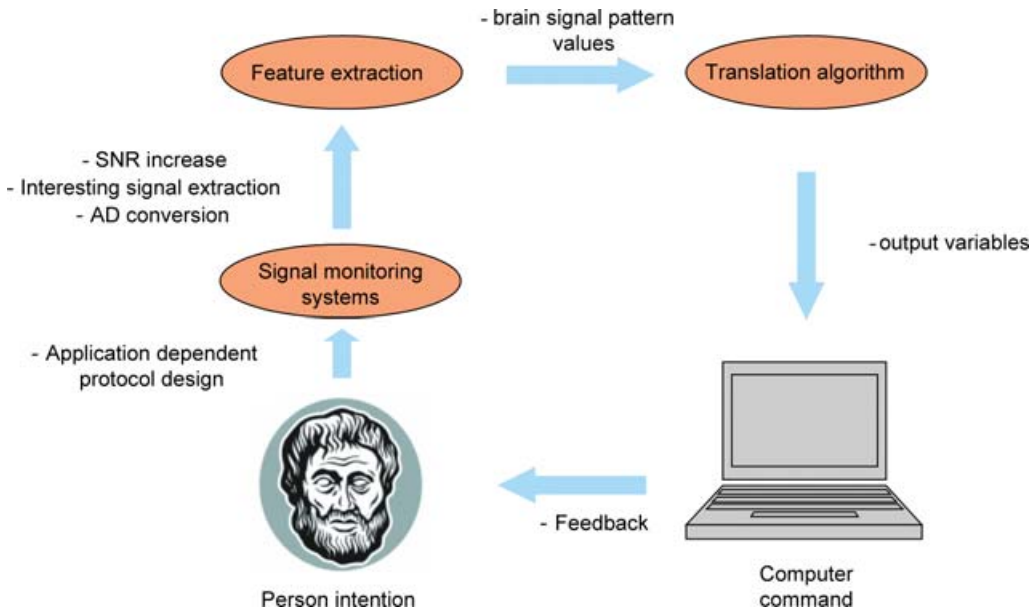

Figure 1. BCI definition
Schematic representation of a BCI. The features that could be improved by the information provided in the present review are indicated in bold.

digitized signal must be analysed further to extract information that is relevant to the mental task under investigation. Before the signals are used, however, often some unwanted artifacts need to be removed. Without exaggeration, thousands of different features have already been used in BCIs, being divided into three general domains: time domain, frequency domain, and joint time–frequency domain. The features are also likely to be location specific.

Mandatory for feature extraction success, the experimental protocol must be designed to suit the application and the environment in which the BCI will be used. This includes choice of mental task, stimulus parameters (e.g. visual scenery timing and constraints), a minimization of unwanted stimuli and distractions that may affect the properties of the signals to be monitored, at list in the first phase of initial algorithm training.

Feature extraction in patients

When developing BCI applications devoted to patients affected by different pathologies, it is mandatory to consider that the cerebral processing is hugely distorted by diseases. For instance, in the case of stroke patients, a relevant phenomenon is that different areas start to replace the function previously played by the damaged areas (plastic modifications characterized by unusual recruitments: Rossini *et al.* 1998, 2001; Oliviero *et al.* 2004; Tecchio *et al.* 2006*d*). In the case of peripheral damage, maladaptive (Flor *et al.* 2006) or adaptive (Tecchio *et al.* 2000*a*, 2002, 2006*d*) cerebral reorganizations can occur (Rossini *et al.* 1994*b*; Tecchio *et al.* 2005*a*, 2006*c*).

Translation algorithms

The relevant extracted features must be transformed into commands directed to the device which has to execute the subject's intentions. This algorithm can be based on linear (e.g. standard statistical methods) or non-linear (e.g. neural networks) techniques. Examples of artificial intelligence methods used are linear discriminant analysis, artificial neural networks, genetic algorithms, kernel-based learning methods (support vector machines, kernel Fisher discriminant), Bayesian networks, and hidden Markov models. In order to be really efficient, an algorithm should adapt to the human subject in at least three phases: (1) initial training of the algorithm, in which BCI adapts off-line to the physiological characteristics of the subject; (2) adaptation by periodic on-line adjustments; (3) mutual adaptation and reinforcement, where the subject's control of the physiological signals used to control the BCI, and the translation algorithm's ability to decode these signals reaches a stable state and an optimization of low error rate is reached.

Learning

Although BCIs provide alternate communication channels that bypass traditional neuromuscular channels, learning to operate a BCI successfully is similar to learning tasks that involve muscular control. Just as walking or speaking requires training and practice, the operation of a BCI is an acquired skill that involves many of the same learning mechanisms. Successful use of BCIs requires that the user maintains his/her capability to learn developing new abilities in controlling not the usual neuromuscular channels, but the EEG pattern that is recognized as relevant by the BCI. Throughout the repeated execution of any task, the brain undergoes plastic adaptation that may be relatively short lived or more persistent. From a system point of view, this plasticity is in essence a transfer function change on the human subject side that inevitably affects the overall behaviour of the BCI and requires adaptation on the machine side as well.

Feedback

The BCI requires the subject learning both during the relevant signal production and translation maintenance. The most important element of such learning is the presence of feedback. During the learning process, either while walking, speaking, or using a BCI, the subject makes adjustments based on the outcomes produced by their own efforts in order to eventually hone their skills appropriately. The incoming signal produced by the outcomes is known as feedback, and it is crucial to the learning process (Graimann *et al.* 2006). As mentioned above, most BCIs feedback to the subject the outputs on a computer monitor. The use of this visual information as feedback presents problems for fast applications. Treisman & Kanwisher (1998) concluded that it takes at least 100 ms after stimulus presentation for sensory perception and nearly another 100 ms for the information to become conscious. This relatively long delay to process conscious information complicates the use of visual feedback as the only one in real-time BCIs, e.g. a system devoted to move an arm in a dynamic and complex situation. Among a number of possible solutions that may be tried in the future to reduce the problems related to perceptual delays, the use of haptic feedback and electrotactile sensations seems to be the most compelling (Graimann *et al.* 2006).

Throughput and latency

Two important numerical parameters that allow the selection of appropriate interfaces for driving specific applications are the throughput and latency. (1) Throughput (also called bitrate, bandwidth, or information transfer rate) is the rate at which a computer or network sends or receives data. It is a good measure

of the channel capacity of a communication link – the throughput unit used in the connections to the internet is how many bits they pass per second (bit s^{-1}). (2) Latency is a time delay between the moment something begins, and the moment its effect begins. Up to now, even the best average information transfer rates for experienced subjects and well-tuned BCI systems are relatively low, in the region of 24 bits min^{-1} (roughly three characters per minute, Wolpaw *et al.* 2002). This is too slow for natural interactive communication, so, to effectively use BCIs as an alternative to conventional interfaces, it is necessary to research ways of optimizing selection techniques and incorporating prediction mechanisms to speed up communication.

Signal-to-noise ratio

Like any other communication channel, the BCI system performance heavily depends on the signal-to-noise ratio (SNR). Feature extraction success depends on the SNR, specifically estimated as the ratio between the occurrence of the wanted (by the subject using the BCI) cerebral signal modulation and the ongoing variation of the same signal in a certain time period. This ratio will affect the translation algorithm efficiency, defined as the ratio between the desired and the produced output. For instance, in a BCI based on sensorimotor cortex mu rhythms, the biological noise includes the alpha activity from other brain areas (e.g. the visual cortex). It is worth noting the importance that BCI systems identify and eliminate signals generated outside the central nervous system, like the electromyography (EMG) from scalp and face muscles and electroculogram (EOG). A further and difficult step is the discrimination of signal from noise if they have similar topography, amplitude and frequency content. For instance, the EOG is more problematic than EMG for those BCI systems operating on the basis of slow cortical potentials (SCP; Birbaumer *et al.* 1999) because of their frequency overlap; similarly beta-dependent BCI systems are more sensitive to EMG artifacts (Goncharova *et al.* 2003).

Brain signal monitoring systems

EEG and MEG (Niedermeyer & Lopes da Silva, 1997; Del Gratta *et al.* 2001) are non-invasive techniques that detect electrophysiological signals with the temporal resolution of a millisecond or better. For both techniques, the origin of the signal is mainly the effect of the postsynaptic currents associated with synchronous neuronal firing in the brain. EEG detects the electrical potential difference measured from the scalp, i.e. it is a reference-dependent measure. It requires the contact between the recording electrodes and the scalp. MEG detects magnetic fields at the cranial surface, giving an absolute measure at each point. The MEG recording system is brought near the head and the sensors are not in contact with the scalp. EEG is equally sensitive to cerebral sources orientated both radially and tangentially to the head surface, whereas MEG is almost selectively sensitive to the latter. Moreover, EEG signal is distorted in space and time by the passage through the conductivity discontinuities of cerebrospinal fluid, meninxes, skull and scalp, while MEG signal is transparent to these discontinuities in the first approximation of spherical head. ECoG (Gastaut, 1952; Keene *et al.* 2000; Allison *et al.* 1991) is the invasive recording of cortical potentials from electrodes placed intracortically or in deep brain regions. With cortical implanted electrodes it allows the mapping of cortical functions; often this investigation is performed intraoperatively, with adjunctive difficulties due to anaesthetics. In humans, ECoG can be used only in pathological conditions requiring neuro-surgery or deep brain stimulation (DBS).

Functional magnetic resonance imaging (fMRI) detects changes in the concentration of deoxyhaemoglobin, dependent on a complex interplay among blood flow, blood volume and cerebral oxygen consumption (Heeger *et al.* 2000; Heeger & Ress, 2002). When neurons increase their activity with respect to a baseline level, a modulation of the deoxyhaemoglobin concentration is induced, generating the so-called blood oxygen level-dependent (BOLD) contrast (Rees *et al.* 2000). BOLD dynamics are characterized by an initial transient small decrease below baseline due to initial oxygen consumption (negative dip), followed by a large increase above baseline, due to an over-supply of oxygenated blood only partially compensated for by an increase in the deoxygenated venous blood volume. The BOLD signal could reflect both the firing of local neuronal assemblies and also the amount of their synchronized input, even if insufficient to evoke an action potential spike, as well as fluctuations in firing synchrony, which can increase or decrease without affecting the net firing rate (Rees *et al.* 2000; Heeger *et al.* 2000). A comparison among different techniques is schematized in Table 1.

This review will focus on cerebral processing features pivotal for feature extraction step in BCI applications aiming at improving hand control. It is formed by two sections. The first will be devoted to the new procedures developed by our group, which can be applied to non-invasive electrophysiological signals (EEG, MEG) to extract the relevant signal useful for BCI feature extraction. In particular, the proposed methods allow identificagtion of specific neuronal pool activity on the basis of proper functional requirements, produce an on-line description of the time course of these neuronal groups – useful to increase throughput and to reduce latency – and select only cerebral physiological activity of interest. Moreover, artifactual signals in phase with the phenomenon of

Table 1. Spatio-temporal characteristics of different brain signal monitoring systems

Technique	Spatial resolution	Temporal resolution	Advantages	Disadvantages
EEG	Poor	Optimal (< 1 ms)	Non-invasive Portable Very low cost Sleep and operation monitoring	Not an imaging technique
ECoG	1 mm	Optimal (< 1 ms)	Low cost Sleep and operation monitoring	Invasive Not an imaging technique
MEG	5 mm	Optimal (< 1 ms)	Non-invasive Excellent signal frequency–temporal characteristics	Very expensive Limited resolution for deep structures
fMRI	3 mm	Low (about 1 s)	Excellent resolution Non-invasive	Expensive Limited to activation studies

interest or much stronger ($> 10^3$) could be removed – producing a SNR increase. The second section will be devoted to organizational changes in the cortical areas devoted to hand control, induced by unilateral stroke within the middle cerebral artery territory, i.e. useful for BCI feature extraction in stroke patients, and to a brief description of the sensorimotor feedback network devoted to the hand control, i.e. useful exploiting of BCI sensory feedback.

Section 1. Functional source separation (FSS)

To ultimately discover and translate the subject's intentions, a BCI starts from cerebral activity as depicted by some brain signal monitoring system. In the case of EEG and MEG, the sensed signal is a linear mixture of source activities. This corresponds to the basic model of the blind source separation (BSS) technique. These algorithms estimate complete source time courses on the basis of the statistical properties of the generated signal, without taking into account the physical nature of the generating phenomenon. Thus, BSS procedures use only information contained in the waveform of original signals, a very convenient property for electrophysiological techniques (EEG and MEG), which provide the most informative time–frequency signal from the intact human brain.

In the last decade the BSS techniques, in particular independent component analysis (ICA) algorithms, have been successfully applied to EEG and MEG data to estimate signal of interest (Makeig *et al.* 1996, 2002, 2004; Vigario *et al.* 1997; Tang *et al.* 2005; for a comprehensive review on BSS see: Hyvärinen *et al.* 2001; Cichocki & Amari, 2002). The aim of such techniques is to extract in a 'blind' fashion (i.e. without making specific assumptions) meaningful signals that have been mixed linearly, without knowing the original signals or the mixing coefficients. There appears to be something magical about BSS; we are estimating the original source signals without knowing the parameters of mixing and/or characteristics of the sources. In fact, without some *a priori* knowledge, it is not possible to uniquely estimate them. However, one can usually estimate them up to certain indeterminacies. In mathematical terms these indeterminacies and ambiguities can be expressed as arbitrary scaling, permutation and delay of estimated source signals. These indeterminacies preserve, however, the waveforms of the original sources. Although these indeterminacies seem to be rather severe limitations, in a great number of applications, like the electrophysiological ones, these limitations are not essential, since the most relevant information about the source signals is contained in their waveforms and not in their amplitudes or in the order in which they are arranged in the output of the system. In particular, the ICA assumption is that a set of statistically independent sources s have been mixed linearly in the recorded data x by means of a mixing matrix A. The aim is to recover both s and A starting from the observation of the linear mixture $x = As$ without making any particular assumption other than statistical independence of the sources.

Based on the observation that when we deal with real-world signals we are never completely 'blind', in that we know (in a more or less detailed and quantitative way) some of their characteristic features, a new approach, called functional source separation (FSS), has been recently proposed by our group (Barbati *et al.* 2006; Porcaro *et al.* 2007). The aim of FSS is to enhance the separation of relevant signals by exploiting some *a priori* knowledge without renouncing the advantages of using only information contained in original signal waveforms. A modified (with respect to standard ICA) contrast function is defined: $F = J + \lambda R$, where J is the statistical index normally used in ICA, while R accounts for the prior information of the sources. According to the weighting parameter λ it is possible to adjust the relative weight of these two aspects. Moreover, since prior information on the sources may also be described by a non-differentiable function, the new contrast function F is optimized by means of simulated annealing. This does not require the use of derivatives, and performs global optimization, while gradient-based algorithms usually employed in ICA only

guarantee local optimization. To separate contributions representing different sources, the proposed procedure could be applied in two different ways: by using an *orthogonal* extraction scheme (as happens in the basic ICA model); after having estimated the first source, the second one is searched in the orthogonal space with respect to the first, and so on until the last source is estimated – with a stop rule that can be defined according to the data in hand. Since relevant components could not always be reasonably assumed independent/uncorrelated, in the FSS procedure the orthogonalization step could be also completely skipped, producing a *non-orthogonal* extraction scheme. In this condition, the order of extraction is not significant, because the procedure is applied each time to the original data. Different constraints are applied each time to produce different sources.

The provided sources are suitable to describe ongoing activity time courses, which allow, for example, single trial analysis, instead of describing the activations by averaging all sensors channels and only in specific instants, as is usually done in the standard procedures. Moreover, even if a source is extracted by exploiting a functional constraint related to a specific time portion of the experiment, the corresponding estimated signal could be studied all along the length of the whole session.

Functional constraints. The described optimization procedure exploits a wide variety of constraints, which express the functional properties, specific to the sources to be estimated (Fig. 2). The BCI applications we are interested in are devoted to the upper limb movements, in particular to the sensorimotor control of the hand. The MEG displays an optimal capability to identify cerebral regions devoted to the hand sensory representation, describing the physiological somatotopic organization (Hari *et al.* 1984; Tecchio *et al.* 1997; Wikstrom *et al.* 1997; Pizzella *et al.* 1999; Zappasodi *et al.* 2006) and its distortion as a consequence of central (Rossini *et al.* 2001; Oliviero *et al.* 2004; Tecchio *et al.* 2005*a*, 2006*c*,*d*) and peripheral damage (Tecchio *et al.* 2002). Moreover, MEG can provide a description of the peripheral–central connectivity of the neural network devoted to the hand (Tecchio *et al.* 2000*b*, 2005*b*).

Primary sensory hand areas. In the case of the primary sensory areas, it is often adequate to exploit the cortical area responsiveness to the stimuli of the corresponding sensory channel at appropriate times. In our FSS applications, we obtained the hand representation areas, in particular the cortical region devoted to the districts innervated by the median nerve and those representing the thumb and little finger of both the hands.

We identified in the primary cortex devoted to the districts innervated by the median nerve two functional sources (FSs) related to the sensory flow induced by median nerve stimulation. The first one – named S1a – describes the activity related to the well-known marker of the stimulus arrival in the primary sensory cortex (Hari & Kaukoranta, 1985; Allison *et al.* 1991). This is known to be mainly generated by excitatory postsynaptic potentials impinging on broadman area (BA) 3b pyramidal cells. As it is maximally recruited at around 20 ms from the stimuli

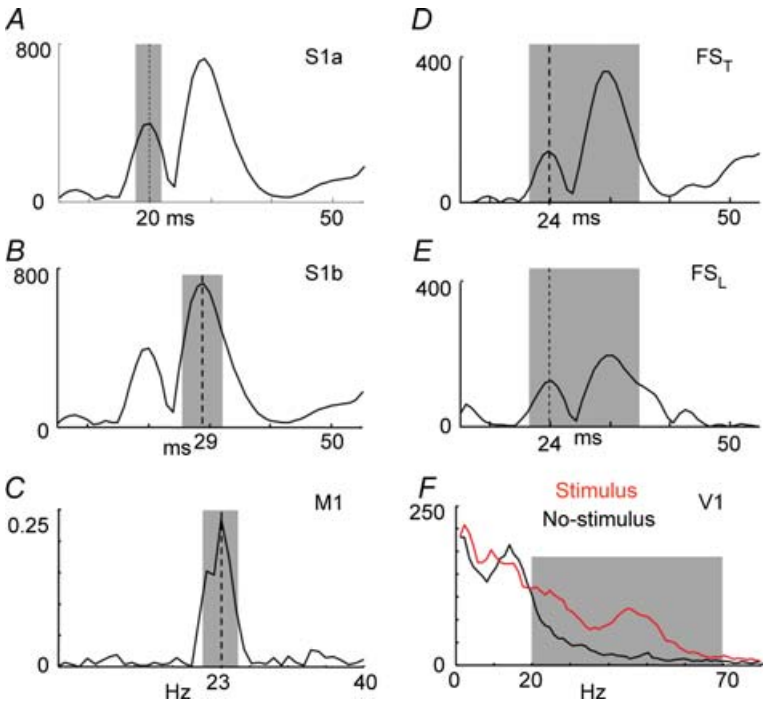

Figure 2. FSS functional constraints
Representation of the quantities maximized by the functional constraint to obtain the FS in our different applications. *A*, FS responsiveness following the contralateral median nerve stimulation. The grey area indicates the time interval around 20 ms where the responsiveness is maximized (corresponding separated source S1a); *B*, as in *A*, with the grey area indicating the time interval around 30 ms where the responsiveness is maximized (obtaining S1b); *C*, cortico-muscular coherence. The grey area indicates the frequency interval around 20 Hz where the cortico-muscular coherence is maximized (obtaining M1); *D*, FS responsiveness following the thumb stimulation. The grey area indicates the time window from 20 to 40 ms where the responsiveness is maximized (FS_T); *E*, evoked activity following the little finger stimulation. The grey area indicates the time window from 20 to 40 ms where the responsiveness is maximized (FS_L); *F*, PSD of the FS in the Stimulus\No-stimulus condition. The grey area indicates the frequency interval from 20 to 70 Hz where the spectral difference between Stimulus and No-stimulus conditions is maximized (obtaining V1). Note that the *y* axes do not have measurable units, as FSs do not have a physical unit dimension, before retro-projection on the original signal space.

at the wrist, the functional constraint taking into account the 'reactivity' to the stimuli to identify S1a was defined as:

$$R_{\mathrm{S1a}} = \sum_{t_{20}-\Delta_1 t_{20}}^{t_{20}+\Delta_2 t_{20}} |\mathrm{EA}(t)| - \sum_{10}^{15} |\mathrm{EA}(t)| \qquad (1)$$

with the evoked activity (EA) computed by averaging source (FS is S1a) signal epochs triggered on the median nerve stimulus at the wrist ($t = 0$); t_{20} is the time point with the maximum magnetic field power on the maximal original MEG channel around 20 ms (searched in the [16–24] ms window) after the stimulus arrival: $\Delta_1 t_{20}$ ($\Delta_2 t_{20}$) is the time point corresponding to a field amplitude of 50% of the maximal power – by definition in t_{20} – before (after) t_{20}; the baseline (no response) was computed in the time interval from 10 to 15 ms. As only one component is extracted at each time, it is possible to avoid the amplitude indeterminacy inherent to the general ICA method. Once the source which optimizes the contrast function F has been obtained, the estimated solution is multiplied by the Euclidean norm of its weight vector $\mathbf{a}_{S1a}$ (a_{S1a} such as $\mathbf{a}_{S1a} = a_{S1a}\hat{\mathbf{a}}_{S1a}$, with $|\hat{\mathbf{a}}_{S1a}| = 1$), allowing amplitude comparisons among sources in a fixed position.

We considered a second cerebral source named S1b, i.e. the source maximally activated in the sensory areas at around 30 ms from nerve stimulation. While invasive recordings using ECoG in human (Allison *et al.* 1991) showed BA 1 at the crown of the postcentral gyrus contributing to this wave of somatosensory-evoked potentials, this radial component is poorly detectable by MEG. The component around 30 ms as recorded by MEG is mainly generated by BA 3b inhibitory and BA 4 excitatory networks (Wikstrom *et al.* 1996; Kawamura *et al.* 1996; Huang *et al.* 2000; Tecchio *et al.* 2005*a*). The functional constraint to obtain S1b was defined as:

$$R_{\mathrm{S1b}} = \sum_{t_{30}-\Delta_1 t_{30}}^{t_{30}+\Delta_2 t_{30}} |\mathrm{EA}(t)| - \sum_{10}^{15} |\mathrm{EA}(t)| \qquad (2)$$

EA was computed as in eqn (1) with FS of S1b; t_{30} corresponded to the maximum magnetic field power on the maximal channel around 30 ms (searched in the [26–36] ms window) after the stimulus arrival; $\Delta_1 t_{30}$ and $\Delta_2 t_{30}$ were as in eqn (1), with t_{30} instead of t_{20}; the baseline was defined as in eqn (1). Again, the estimated solution was multiplied by the Euclidean norm of its weight vector $\mathbf{a}_{S1b}$ (a_{S1b} such as $\mathbf{a}_{S1b} = a_{S1b}\hat{\mathbf{a}}_{S1b}$, with $|\hat{\mathbf{a}}_{S1b}| = 1$).

Primary sensory finger areas. To identify neural networks devoted to individual finger central representation, the 'reactivity' to the stimuli was taken into account in the whole period including the two early components. It was defined as follows: the evoked activity (EA) was computed separately for the two sensorial stimulations by averaging signal epochs centred on the corresponding stimulus ($\mathrm{EA_L}$, little finger; $\mathrm{EA_T}$, thumb). The reactivity coefficient (R_{stim}) was then computed as:

$$R_{\mathrm{finger}} = \sum_{t=20}^{40} |\mathrm{EA}_{\mathrm{finger}}(t)| - \sum_{t=-30}^{-10} |\mathrm{EA}_{\mathrm{finger}}(t)| \qquad (3)$$

with finger = thumb (T), little finger (L) and $t = 0$ corresponding to the stimulus arrival. The time interval ranging from 20 to 40 ms includes the maximum activation (Allison *et al.* 1980; Tecchio *et al.* 1997) and the baseline (no response) was computed in the prestimulus time interval (−30 to −10 ms). To estimate the time behaviour of the neural networks devoted to the thumb ($\mathrm{FS_T}$) and little finger ($\mathrm{FS_L}$) cortical representations during different activation states, each functional source was extracted using data along the entire recording period, alternating these two fingers and median nerve separate stimulation.

As already mentioned, the orthogonality constraint was removed and the two finger sources were searched for starting from the original data. In fact, in the specific and restricted cortical region of interest, neural networks are spatially highly interconnected and superimposed and temporal overlap of finger sources activation could be reasonably hypothesized.

Primary visual sustained induced activity. In the visual cortex, to observe the cerebral activity induced by a sustained stimulus, the robust and temporally induced power increase of gamma activity was exploited, by the spectral power band relative variation during the whole period of sustained stimulus and the period of stimulus absence. The following ad hoc functional constraint R was:

$$R_{V1} = \frac{\sum_{\gamma} \mathrm{PSD}_{\mathrm{Stimulus}} - \sum_{\gamma} \mathrm{PSD}_{\mathrm{No\text{-}stimulus}}}{\sum_{\gamma} \mathrm{PSD}_{\mathrm{No-stimulus}}} \qquad (4)$$

by computing the PSD (power spectrum density) area difference of the source (FS) between stimulus (from 0 to 4.5 s of each trial, $t = 0$ corresponding to the stimulus onset) and No-stimulus (from −4.5 to 0 s of each trial) in the γ (gamma, 20–70 Hz) frequency band and normalizing this difference with respect to the gamma activity level at No-stimulus (Barbati *et al.* 2007).

Primary motor hand area. To identify the source in the primary motor area devoted to the control of the hand movements – named M1, the coupling of cortical and muscular rhythmic oscillations in the beta band was taken into account. In fact, it has been demonstrated that the component of the synchronized cortical activity, coupled to synchronous rhythmic motor-unit firing – assessed by surface EMG – within this band, characterizes aspects of cortical control on voluntary movement (Conway *et al.* 1995; Gross *et al.* 2000; Kilner *et al.* 2000), and

is generated in the primary motor cortex (Brown *et al.* 1998; Brown, 2000; Gerloff *et al.* 2006*a*). A component of the synchronized cortical activity has been demonstrated coupled to synchronous rhythmic motor-unit firing assessed by EMG surface recordings both in animals and humans (Piper, 1907, 1912; Baker *et al.* 1997). In monkeys, for example, pyramidal neurons of the primary motor cortex show bursts of oscillations in the beta band during a precision grip task, coupled with the rectified EMG of the active muscles (Murthy & Fetz, 1992). MEG has provided the first direct extra-cephalic measurement of such cortical–muscular oscillation coupling (Conway *et al.* 1995). This technique has shown systematic cortico-muscular coherence related to the patterns of motor output and sensory input, both in healthy subjects (Gross *et al.* 2000; Brown & Marsden, 2001; Kristeva-Feige *et al.* 2002; Tecchio *et al.* 2006*a*) and in patients with motor disorders (Brown *et al.* 1998, 1999; Volkmann *et al.* 1996; Timmermann *et al.* 2003; Kristeva *et al.* 2004). The corresponding functional constraint to obtain the M1 source was:

$$R_{\mathrm{M1}} = \sum_{\omega_{\max}-\Delta_1\omega_{\max}}^{\omega_{\max}+\Delta_2\omega_{\max}} Coh(\omega) \qquad (5)$$

where C*oh* is a function of frequency ω, obtained for each ω as the amplitude of the cross-spectrum between the M1 source signal and the rectified EMG, normalized by the root mean square of the power spectral densities of these two signals; $\Delta_1\omega_{\max}$ ($\Delta_2\omega_{\max}$) is the frequency point corresponding to a coherence amplitude of 50% of the maximal value between [13.5–33] Hz – called $\omega_{\max}$ – before (after) $\omega_{\max}$. As for S1a and S1b, M1 was obtained by multiplying it by the Euclidean norm of its weight vector $\mathbf{a}_{\mathrm{M1}}$ (a_{M1} such as $\mathbf{a}_{\mathrm{M1}} = a_{\mathrm{M1}}\hat{\mathbf{a}}_{\mathrm{M1}}$, with $|\hat{\mathbf{a}}_{\mathrm{M1}}| = 1$).

The FSS algorithm is flexible allowing exploit of different constraints, also not differentiable as simulated annealing is the optimization procedure. The functional constraint could be defined suitably for the experimental conditions in use. In our examples, the static visual stimuli induce a power increase in the gamma band sustained along the stimuli duration, a response more evident than the visual evoked field. This latter point can be exploited in the functional constraint if flashing lights or pattern reversal are used as visual stimuli. For the primary motor area identification, the motor task we used was an isometric contraction for periods of about 20 s, inducing a significant synchronization between primary motor and electromyographic activities in the beta band and the constraint was chosen accordingly (maximization of MEG–EMG coherence). For this area identification the motor-related fields or potentials would be the suitable functional constraint if the motor task were the abrupt repetitions of a body district movement.

FS evaluation. The estimated FSs in all cases contained practically all the required signal features, demonstrating the ability to describe the dynamics of different primary cortical network responsiveness, primary visual sustained activity or primary motor synchronization phenomena (Fig. 3).

Although the FSS constraints allow identification of sources only on the basis of their function behaviour, the generated field distribution could be obtained by retro-projecting the source activity in the sensor space and could be used as the input for inverse-problem solution algorithms. The sources were in all cases positioned in agreement with well-established anatomical knowledge (Fig. 4 left).

FS functional behaviour. The sources extracted requiring a characteristic functional property in a specific time period, are obtained along the whole experimental session, including all the planned experimental conditions (Barbati *et al.* 2006; Porcaro *et al.* 2007; Tecchio *et al.* 2007*a*; Barbati *et al.* 2007). To give an example, we observed all the FSs in the hand sensorimotor area (S1a, S1b, FS_T, FS_L, M1; Fig. 4) during the stimulation of the median nerve. We observed that FS_T showed a higher responsiveness to the median nerve stimulation with respect to the thumb stimulation itself (Barbati *et al.* 2006), in agreement with the physiology of the hand innervation. In fact, it is well known that in stimulating a nerve directly, all the proprioceptive and the superficial perception fibres of innervated districts are recruited; therefore, the cerebral source representing the thumb – innervated by the median nerve – is expected to be more reactive to the stimulation of this nerve with respect to the cutaneous stimulation obtained by ring electrodes. Moreover, median nerve stimulation over the motor threshold induces a partial stimulation of the ulnar nerve (innervating the little finger) and consequently of the little finger proprioceptive and superficial perception fibres (FS_L in Fig. 4; Barbati *et al.* 2006). Another interesting property, emerging in the FS behaviour without being required by the functional constraint, was that M1 reacted to galvanic median nerve stimulation more at around 30 ms than at 20 ms (Fig. 4; Porcaro *et al.* 2007). This last property sustains a contribution from precentral neuronal pools in originating M30 component (BA 4; Kawamura *et al.* 1996; Tecchio *et al.* 1997, 2005*b*; Huang *et al.* 2000).

We give these examples to show the FS potential to be obtained exploiting a specific functional requirement in a specific time period and to be afterwards used to describe the behaviour of the neuronal pool identified with the specific functional property, in different experimental stages. In relationship with BCI, this property could be exploited in two main ways. The weight vector obtained in one session can be used in successive recordings. In this regard, our experience (authors' unpublished data) indicated that a suitable description is obtained if

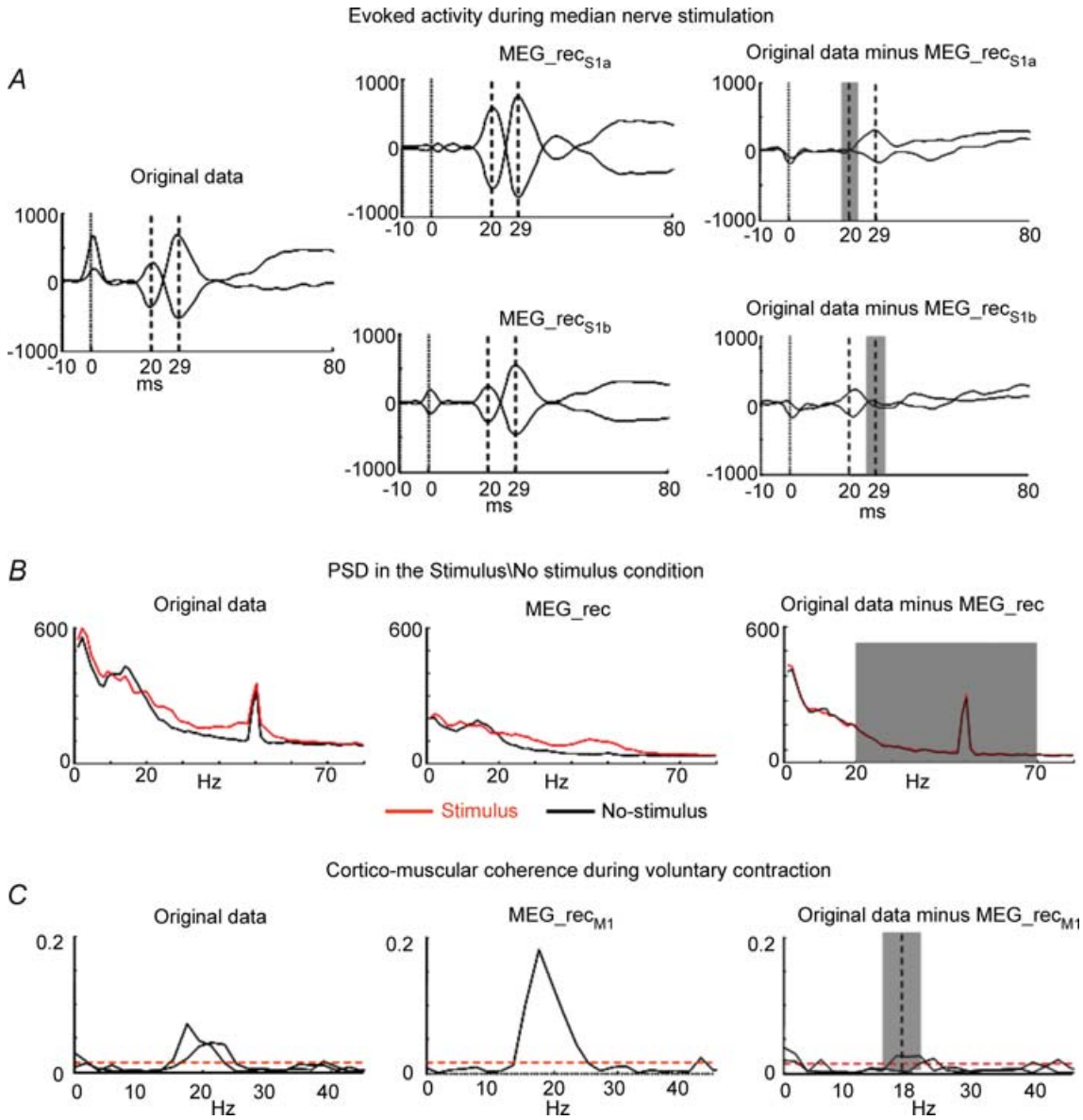

Fig. 3. FS discrepancy

A, evoked activity during median nerve stimulation. In one representative subject, the two most representative parietal channels are superimposed in the time window [−10, 80] ms, after averaging on median nerve stimuli, $t = 0$ being the stimulus arrival at wrist (vertical continous line). The time points corresponding to M20 and M30 components are indicated (vertical dashed lines). Left: original data. Centre: retro-projected data with only the S1a source (top, MEG·rec$_{S1a}$) and with only the S1b source (bottom, MEG·rec$_{S1b}$). Right: original data minus MEG·rec$_{S1a}$ (top) and original data minus MEG·rec$_{S1b}$ (bottom). The grey area indicates the time interval ($\Delta_2 t_{20} + \Delta_1 t_{20} + 1$ top, $\Delta_2 t_{30} + \Delta_1 t_{30} + 1$, bottom) where the functional constraint, i.e. the FS responsiveness, is maximized. Note that both S1a and S1b well explain the generated field at their respective latencies. *B*, PSD in the Stimulus\No-stimulus condition. Left: PSD of one representative MEG sensor signal in the occipital region displayed in the frequency window [0, 80] Hz. Centre: retro-projected channel with the estimated FS (MEG·rec). Right: PSD of the original MEG data minus MEG·rec channel. The grey area indicates the frequency interval [20, 70] Hz) where the functional constraint, i.e. the band power difference between Stimulus and No-stimulus conditions, is maximized. *C*, cortico-muscular coherence during voluntary contraction. The two channels most coherent with electromyographic activity are chosen. Their coherences with the rectified EMG in the frequency window [0, 45] Hz. The confidence limit is indicated (0.015, horizontal dashed line). Left: original data. Centre: retro-projected channels with only M1 (MEG_rec$_{M1}$). The two channels display the same coherence with the EMG signal, as all the channels obtained by retro-projecting only one FS display the same time evolution, unless a multiplicative factor and the coherence is independent from the signals amplitude. Right: original MEG data minus MEG_rec$_{M1}$ channels. The grey area indicates the frequency interval ($\Delta_2 \omega_{max} + \Delta_1 \omega_{max} + 1$) where the FS–muscular coherence (dimensionless) is calculated.

similar conditions occur (weight vectors extracted from similar experimental sessions in different days display correlations higher than 0.91); it would be of high interest to confirm these preliminary positive findings in FS components extracted from a controlled laboratory setting, later applied to a noisy real-world environment, where competing processes should be expected. The second opportunity is to use the weight vector to isolate the activity from a specific neuronal pool, in this way being more sensitive to volitional modulations of the activity from those areas. For example, the selection of the activity from primary visual areas by the above described functional constraint, could allow more sensitivity to volitional visual imagery.

ICA artifact removal. Muscle contraction on the cephalic district as well as eye movements produce electromagnetic signals which can be recorded from scalp electrodes with amplitudes that can easily overwhelm the brain generated signals, particularly on frontal, temporal and occipital regions (McFarland *et al.* 1997; Anderer *et al.* 1999; Croft & Barry, 2000; Goncharova *et al.* 2003). More importantly, the EMG signal from frontal muscles can imitate the frequency of the mu and beta rolandic rhythms and the electro-oculographic (EOG) signal and blinking can resemble the fronto-central theta rhythms. Although FSS could in principle be successful even in the presence of disturbance signals, if they are uncorrelated with the required functional characteristics expressed in the functional constraint, on some occasions, artifactual activities could be as higher as 10–100 times stronger than the signal of interest or be in phase with it (Goncharova *et al.* 2003). In these cases, it could be very helpful to previously identify and discard these artifacts. ICA was proven to be an efficient procedure to remove artifactual activity avoiding trails exclusion (Vigario *et al.* 1997; Ziehe *et al.* 2000, 2001; Cao *et al.* 2000; Delorme & Makeig, 2004). We introduced a suitable strengthening and simplification of ICA preprocessing data analyses, through an automatic detection system of artifactual components (ICs), based on statistical and spectral ICs characteristics (Barbati *et al.* 2004). Moreover, the procedure allows recovery of part of the non-artifactual signals possibly lost by the blind mechanism, via a control cycle on the difference between original data and those reconstructed using only ICs automatically retained. This step, after automatic pruning, seems to be a suitable way to render negligible the risk of loose non-artifactual activity when applying BSS methods to real data. An emblematic case of artifacts 50–100 times larger than the signal of interest comes from MEG fetal recordings, where the cerebral activity of the fetus is largely overwhelmed by the magnetic signal generated by mother heartbeat and partly by the fetal one. In this case, we developed an ad hoc functional selection procedure of ICs, removing the maternal and fetal cardiac activities, so disclosing the fetal auditory responses to the external sound stimulation (Porcaro *et al.* 2006; Fig. 5).

As we saw above, researchers in the BCI field have attempted to set up experimental protocols and analysis

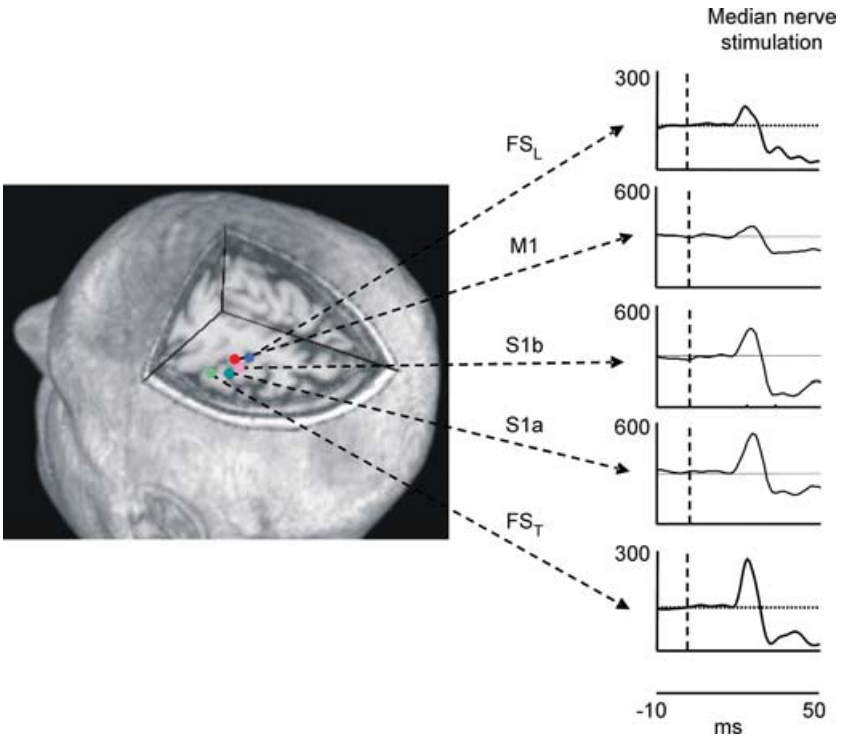

Figure 4. FS positions and behaviour
Left, position in one representative subject of extracted sources representing the thumb cortical network (FS_T), the median nerve connected sensory areas (S1a, S1b), the primary motor area (M1) and the little finger cortical network (FS_L) in the left hemisphere projected on a representative axial section. Right, dynamics of FS_L, S1a, S1b, M1 and FS_T activities during contralateral median nerve stimulation, shown after averaging the source signal timed on the stimulus onset ($t = 0$, vertical dashed line) in the [−10, 50] ms time window. Note that S1a responsiveness is maximal around 20 ms, S1b around 30 ms, and M1 responded more at 30 ms than at 20 ms (see text). Note that the *y* axes do not have measurable units, as FSs do not have a physical unit dimension, before retro-projection on the original signal space.

procedures to increase throughputs and decrease latencies (Xu *et al.* 2004; Lee *et al.* 2006). Up to now, BSS algorithms have been applied in BCI to enhance the feature extraction in motor imagery (Makeig *et al.* 2000; Qin *et al.* 2004; Hung *et al.* 2005), visually induced (Lee *et al.* 2006) and cognitive (Culpepper & Keller, 2003; Xu *et al.* 2004; Serby *et al.* 2005) tasks. The BSS community is also strongly involved in developing online procedures (Serby *et al.* 2005; Piccione *et al.* 2006). Since FSS returns the single trial time courses of the source of interest without requiring the selection between several components, it could be an even more promising tool.

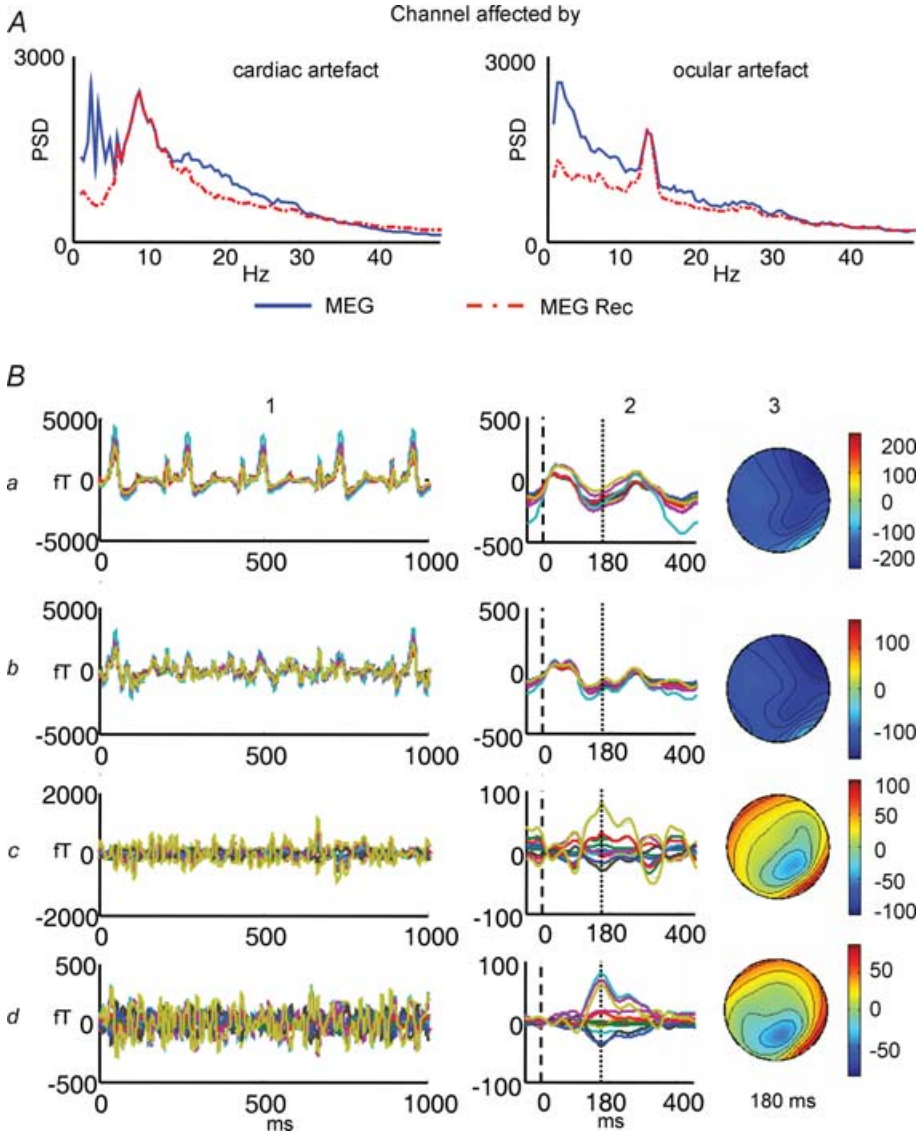

Figure 5. ICA artifact removal
A, PSD of two channels overlapped before (continous blue line) and after (dotted line) artifacts rejection. The left channel is chosen as it is much sensitive to cardiac artifact, and the right one to ocular artifact. *B*, effects of the ad hoc IC artifact removal and IC functional selection procedure. All MEG sensors overlying the fetus head are superimposed. Column 1: signal during a 2 s time period; column 2: signal average on the external sounds (dotted vertical line); column 3: spatial magnetic field distribution at the latency of the main component (continous vertical bar). *a*, original MEG filtered signals: maternal and fetal cardiac peaks are evident in the trace. *b*, retro-projection of all ICs but those describing the maternal cardiac activity. *c*, retro-projection of all ICs but those describing the maternal and fetal cardiac activity; average in *c*2 still shows a poor quality of morphology, as auditory response latency and amplitude are not identifiable. *d*, retro projection of only the ICs describing the auditory response, according to the ad hoc procedure. Latency and amplitude of the auditory response are now clearly identifiable (*d*2). In this case, the field distribution (*d*3) shows a dipolar-like shape, indicating a good positioning of the system with respect to the fetus head.

FSS comparison with other source identification methods. The main difference between FSS and the other source identification methods, ranging from inverse problem-solving algorithms (single and multiple dipoles: Scherg & Berg, 1991; Multiple Signal Classification (MUSIC): Mosher *et al.* 1992; recursively applied and projected-MUSIC (RAP-MUSIC): Mosher & Leahy, 1999; minimum norm estimates: Hämäläinen & Ilmoniemi, 1994; Low resolution brain electromagnetic tomography (LORETA): Pascual-Marqui *et al.* 1995) to spatial filtering like beam forming (for example synthetic aperture magnetometry, (SAM): Vrba & Robinson, 2001), is that no information about the physical relationship between cerebral source generators and generated field distribution is taken into account. Separated FSs provide the source activities in time and the spatial distribution of the field they generate, from which appropriate modelling can to be used to solve the inverse problem to know the source position. The solution of the inverse problem theoretically provides in one go both the source position and its time evolution. Unfortunately, on one side it is hill posed and adjunctive information is to be added, chosen properly time by time. On the other side the solution is based on the relationship, described by the Maxwell equations, between the current distribution and that of the generated field. This relation depends on physical properties, i.e. the shape of conductor volume (the head), the distribution and cytoarchitecture of the cerebral regions (place of the currents generating the field), the geometrical characteristics and conducibility values of the extra-cerebral tissues (cerebrospinal fluid, meninxs, skull, scalp) none of which are known with precision. As a consequence, the inverse problem solution is based on information less accurate provided by the electrophysiological techniques, while FSS algorithms do solve the source identification problem using the most accurate information, i.e. the statistical temporal frequency properties of the signal. As we said before, once the source has been identified, to know its position the proper inverse problem solution can be calculated. In many cases, the scientific interest is in the morphological and temporal characteristics of the signal and its modulation in the different experimental conditions, and the inverse problem solving step is not necessary. Whenever the source position is of specific interest, the advantage is in applying localization algorithms having isolated the field distribution generated by the specific source only.

Section 2. Hand sensorimotor organization and its changes in stroke patients

Many years of research in functional imaging has documented that the ultimate factor sustaining recovery is, in parallel with the 'awakening' of neurons in the perilesional zone of ischaemic penumbra (Heiss & Graf, 1994), the neural ability to change the properties of the activation induced by inputs from peripheral receptors and/or other brain areas. This ability is called cerebral plasticity (for review see Calautti *et al.* 2003; Rossini *et al.* 2003; Hummel & Cohen, 2005). When setting up BCI feature extraction, these cerebral reorganizations should be taken into account, especially in the electrophysiological counterpart, since EEG and MEG are the brain signal monitoring systems best suited for most realistic BCIs. In particular, MEG is especially suitable in poststroke studies, because the morbid tissue near the cerebral generators has minimal effects on the scalp distribution of the magnetic field (Huang *et al.* 1990; Maclin *et al.* 1994). BCI feature extraction is based on two main steps: spatial identification of the interesting signal sources and the time–frequency characterization of this signal. To guide BCI applications, it is expected that the activity from the areas positively contributing to the clinical recovery are the most appropriate and informative. In patients affected by a monolateral ischaemic lesion in the middle cerebral artery territory inducing a sensorimotor impairment of the upper limb, a diverse contribution to the clinical recovery by several area reorganizations in the affected (ipsi-lesional ILH) and the unaffected hemisphere (contra-lesional CLH) is going to be recognized. The activation of CLH non-primary motor areas was reported to decrease proportionally with the improvement of motor performance (Calautti & Baron, 2003; Schaechter, 2004) and CLH SM1 activations were commonly considered as a marker of poor recovery (Loubinoux *et al.* 2003; Calautti *et al.* 2003). Conversely, increasing findings support a positive role of non-primary ILH areas in patients recovering incompletely (Johansen-Berg *et al.* 2002; Loubinoux *et al.* 2003; Fridman *et al.* 2004; Gerloff *et al.* 2006*b*). Moreover, a similar hypothesis was suggested for the recruitment of ILH areas excessively asymmetrical from homologous in the CLH (Pineiro *et al.* 2001; Calautti *et al.* 2003; Thickbroom *et al.* 2004). On the basis of the symmetrical organization of primary hand areas, demonstrated by different techniques in healthy subjects (Rossini *et al.* 1994*b*; Puce *et al.* 1995; Hallet, 1996; Tecchio *et al.* 1997; Wikstrom *et al.* 1997), the comparison of the ILH to the CLH in mono-hemispheric stroke patients allows a sensitive procedure to identify reorganization phenomena in the damaged cerebral regions. On this basis, an ad hoc procedure was previously introduced, for the identification of excessive interhemispheric asymmetries of primary sensory hand areas (Tecchio *et al.* 1997, 2000*b*, 2005*b*). In these studies, a galvanic median nerve stimulation was used, a protocol especially suitable in patients because it equals the input to the two hemispheres. It seems, for this reason, more appropriate in order to detect interhemispheric recruitment asymmetries of homologous areas, with respect to active motor tasks (Kotani *et al.* 2004) where the functional demand to control the paretic and non-paretic hand cannot be equalled. In patients in stabilized conditions (more

than 1 year from symptoms onset), primary sensory cortical hand areas topographical modifications and responsiveness amplitudes were observed (Rossini *et al.* 1998, 27 patients; Rossini *et al.* 2001, 17 patients), with brain areas outside the normal boundaries and usually not reached by a dense sensory input from the opposite hand acting as somatosensory hand centres. These mechanisms were linked with the hand sensorimotor recovery (Rossini *et al.* 1998, 2001; Tecchio *et al.* 2006*d*; Altamura *et al.* 2007). A deeper knowledge of brain mechanisms sustaining recovery in stroke patients who do not achieve a normal neurological function by standard procedures, is of utmost importance, since this group could best benefit from adjunctive rehabilitative-stimulating interventions, like BCI-mediated procedures.

Once spatial properties of interesting signal sources have been identified, BCI will exploit their time–frequency characteristics. When studying rest activity in post-acute and chronic phase, perilesional delta activity was commonly observed (Butz *et al.* 2004, 23 patients). Moreover, frequency-selective alterations related to specific dysfunctions were found: global clinical status was mostly impaired in patients with increased total and slow band activity powers, whereas hand functionality was mostly disrupted in patients with a reduction of high-frequency rhythms (Tecchio *et al.* 2006*c*, 56 patients; Tecchio *et al.* 2006*c*, 32 patients).

While all the above mentioned studies are most suitable to characterize recruitment changes in patients, the organization of the movement control remains the ability the BCI tools should help to recover. Motor imagery is a protocol design also suitable for patients with more severe movement impairment. It is clearly indicated by the literature that the brain activity subtending motor imagery is modified in patients (Sharma *et al.* 2006). In healthy subjects, movement imagery can focus specific facilitation on the prime-mover muscle for the mentally simulated movement (Rossi *et al.* 1998*a*) and mental simulation affects spinal motoneuronal excitability as well, although it has been proved that the main effect takes place at cortical level (Rossini *et al.* 1999). Reviews considering motor imagery in healthy subjects and in patients with stroke – which may disrupt the motor imagery network – suggested the encouraging effect of motor imagery training on motor recovery after stroke (Lotze & Cohen, 2006; Sharma *et al.* 2006). While in healthy volunteers, robust activation of the non-primary motor structures, but only weak and inconsistent activation of M1 occurs during motor imagery, in patients with stroke, the cortical activation patterns are proved to involve M1 in both the affected and unaffected hemispheres (Cicinelli *et al.* 2006). These results indicate that if an appropriate methodology is implemented, motor imagery may provide a valuable tool to access the motor network for BCI feature extraction in stroke patients.

As mentioned above, the computer-mediated visual feedback presents problems for fast applications, while the haptic feedback and electro-tactile sensations present more realistic timing. All studies devoted to the organization of the sensory and proprioceptive inflow underline that a successful motor control relies on the continuous and reciprocal exchange of information between activities of motor areas involved in the task program execution and those elaborating proprioceptive sensory information (Terao *et al.* 1999; Scott, 2004). As a matter of fact, subjects with complete deprivation of proprioceptive feedback (such as in some cases of peripheral neuropathy) can move their limbs using visual feedback (e.g. by looking at the limb), but their movements are typically sluggish, coarse, require substantial mental concentration and attention, and corrections are therefore delayed and often cause other mistakes (Sainburg *et al.* 1998; Gordon *et al.* 1995).

Short-term influences on motor cortical organization have been demonstrated by modification of sensory input both in animal experiments and in healthy humans by using several types of technology for functional brain imaging (Brazil-Neto *et al.* 1992; Rossini *et al.* 1994*a*; Sadato *et al.* 1995; Kristeva-Feige *et al.* 1996). Mechanisms of rapid anaesthesia-related perturbation with changes occurring at multiple levels of sensory system somatotopy were proven (Nicolelis *et al.* 1993), underlying the intimate relationship between primary sensory and motor regions. Experimental findings speak in favour of a significant role played by the tonic sensory flow from the skin receptors and from the phalangeal joint receptors in energizing the corticospinal tracts governing muscles (Johansson & Westling, 1987; Rossini *et al.* 1996*a*, *b*; Rossi *et al.* 1998*b*). For BCI applications, such evidence indicates the need to substitute with compensating feedback mechanisms the absence of the physiological one, to obtain a satisfactory movement control.

To optimize knowledge on proprioceptive information properties in the region dedicated to hand control, we investigated the primary sensory and motor cortices interactions, obtaining a simultaneous assessment of sensory cortex activity modulation due to movement and of motor cortex activity modulation due to sensory stimulation (Tecchio *et al.* 2006*b*; Fig. 6). The introduced protocol is repeatable and suitable for patients, thus it is suitable to investigate patients eligible for BCI applications. In fact, primary sensory cortical excitability is indexed by the most repeatable and subject attention-independent components of brain response to the median nerve stimulation at the wrist (Hari & Kaukoranta, 1985; Allison *et al.* 1991). A relative high-frequency nerve stimulation (around 2 Hz) was used to reduce the recording time. The primary motor cortex contribution to movement control is indexed by cortico-muscular coherence (Brown *et al.* 1998) requiring a motor task both as simple and common

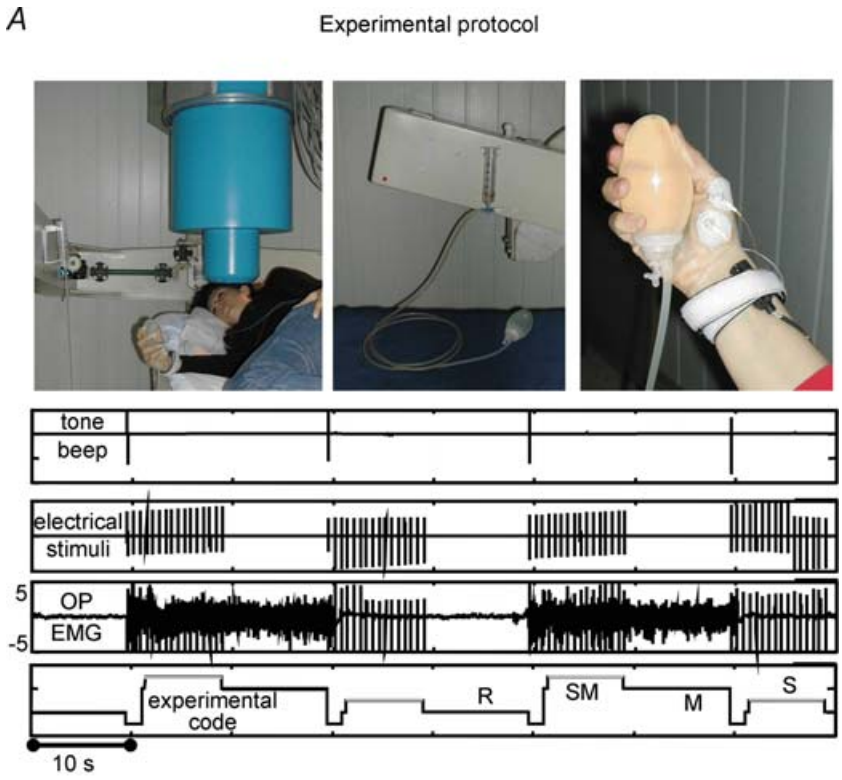

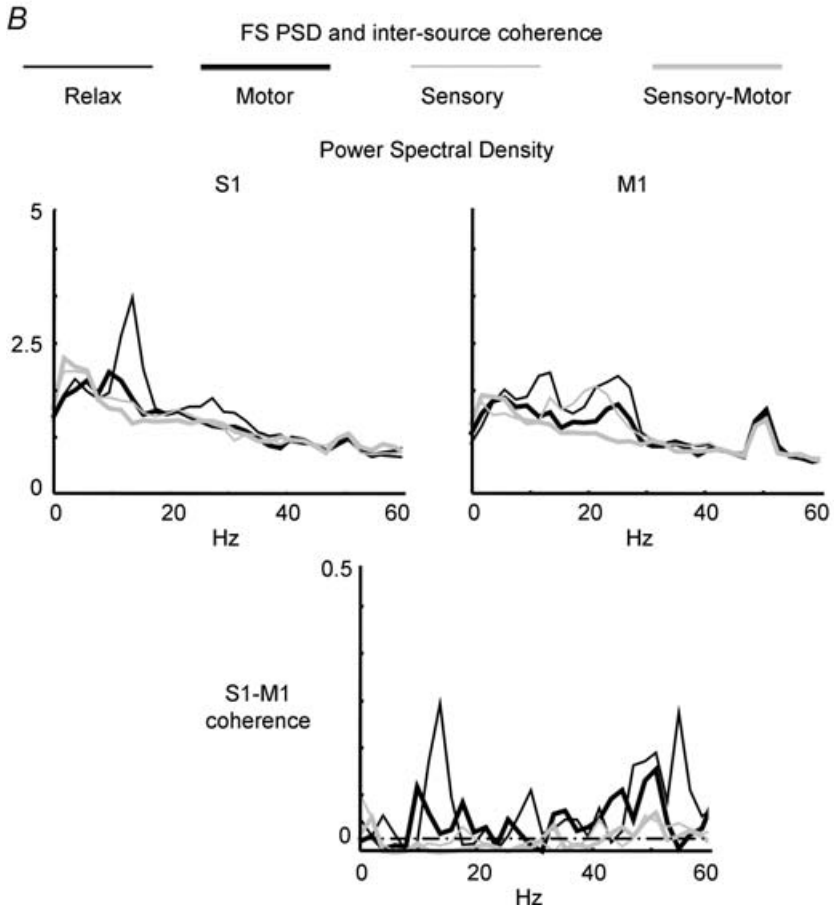

Figure 6. Sensorimotor feedback
A, experimental protocol: Top from left: (1) subject position during recordings from scalp positions overlying the peri-rolandic area contra-lateral to the moved-stimulated hand: (2) non-magnetic device, i.e. the water sphygmomanometer, to control the level of contraction: (3) showing the thumb position during isometric contraction, with electrodes recording OP EMG signal, as well as the median nerve stimulation at wrist. Bottom from top: (1) trigger indicating tone beep for starting/stopping isometric contraction: (2) trigger indicating sensory stimuli to the median nerve at wrist: (3) electromyographic signal, where relax and contraction periods are clearly noticeable, as well as the sensory stimuli artifact: (4) off-line generated signal code differentiating the 4 experimental conditions: relax (R), sensory (S), motor (M), sensory-motor (SM). *B*, FS PSD and intersource coherence. PSD of the S1 and M1 cerebral sources (top) and S1–M1 coherence (bottom) in the four experimental conditions in a representative subject. Note: higher S1 representation in the alpha band and higher M1 beta and gamma band representation; lower S1–M1 coherence in all condition with respect to rest in the three frequency bands and values above significance threshold in motor condition (dashed–dotted line). Note that the *y* axes of S1 and M1 PSDs do not have measurable units, as FSs do not have a physical unit dimension. The S1–M1 coherence is a dimensionless quantity.

as possible, thus most suitable in patients with upper limb impairments. In fact, the experimental contraction is preserved to extremely severe movement impairments, e.g. in diseases affecting the hand motor control, like stroke and Parkinson's disease or hand dystonia. As described in Section 1, the ad hoc FSS was developed to extract S1 and M1 source activities (Porcaro *et al.* 2007), allowing characterization of the spectral properties, the functional involvement of S1 and M1 and their coupling in the above described sensorimotor tasks (Fig. 6). It could be very useful to reveal alterations in pathological conditions and setting up feedback control systems for BCI use.

Conclusions

Our review presents innovative methods expected to enhance BCI feature extraction from EEG or MEG signals, for applications devoted to improve hand control. In particular, the provided experimental set-up and analysis tools could be used to ameliorate a BCI system. In fact, they increase the signal-to-noise ratio by removing non-cerebral artifacts even when they are many times (10–100) larger than the signal of interest. Moreover, they offer a procedure to extract exclusively the sources of interest, obtaining their time course along with the whole experimental session on the basis of appropriate functional requirements taking place in specific time periods. Since the FSS procedure is suitable for single trial analysis, it is promising for online developments – increasing BCI throughput and reducing latency. For applications in patients, information about the recruitments of unusual areas to control the hand were provided, useful for both protocol design definition and interesting signal extraction. Finally, information about primary sensory and motor area relationship was introduced, as a first step to use the haptic feedback and electrotactile sensations which have been indicated as the most compelling for BCI applications aiming at improving hand movement control.

References

Allison T, Goff WR, Williamson PD *et al*. (1980). On the neural origin of the early components of the human somatosensory evoked potentials. In *Progress in Clinical Neurophysiology*, ed. Desmedt JD, pp. 51–68. Karger, Basel.

Allison T, McCarthy G, Wood CC *et al*. (1991). Potentials evoked in human and monkey cerebral cortex by stimulation of the median nerve. A review of scalp and intracranial recordings. *Brain* **114**, 2465–2503.

Altamura C, Torquati K, Zappasodi F *et al*. (2007). fMRI-vs-MEG evaluation of post-stroke interhemispheric asymmetries in primary sensorimotor hand areas. *Exp Neurol* in press.

Anderer P, Roberts S, Schlögl A *et al*. (1999). Artifact processing in computerized analysis of sleep EEG – a review. *Neuropsychobiology* **40**, 150–157.

Baker SN, Olivier E & Lemon RN (1997). Coherent oscillations in monkey motor cortex and hand muscle EMG show task-dependent modulation. *J Physiol* **501**, 225–241.

Barbati G, Porcaro C, Hadjipapas A *et al*. (2007). Functional source separation applied to induced visual gamma activity. *Hum Brain Mapp* in press.

Barbati G, Porcaro C, Zappasodi F *et al*. (2004). Optimization of an independent component analysis approach for artifact identification and removal in magnetoencephalographic signals. *Clin Neurophysiol* **115**, 1220–1232.

Barbati G, Sigismondi R, Zappasodi F *et al*. (2006). Functional source separation from magnetoencephalographic signals. *Hum Brain Mapp* **27**, 925–934.

Birbaumer N, Ghanayim N, Hinterberger T *et al*. (1999). A spelling device for the paralysed. *Nature* **398**, 297–298.

Brasil-Neto JP, Cohen LG, Pascual-Leone A *et al*. (1992). Rapid reversible modulation of human motor outputs after transient deafferentation of the forearm: a study with transcranial magnetic stimulation. *Neurology* **42**, 1302–1306.

Brown P (2000). Cortical drives to human muscle: the Piper and related rhythms. *Prog Neurobiol* **60**, 97–108.

Brown P, Farmer SF, Halliday DM *et al*. (1999). Coherent cortical and muscle discharge in cortical myoclonus. *Brain* **122**, 461–472.

Brown P & Marsden JF (2001). Cortical network resonance and motor activity in humans. *Neuroscientist* **7**, 518–527.

Brown P, Salenius S, Rothwell JC *et al*. (1998). Cortical correlate of the Piper rhythm in humans. *J Neurophysiol* **80**, 2911–2917.

Butz M, Gross J, Timmermann L *et al*. (2004). Perilesional pathological oscillatory activity in the magnetoencephalogram of patients with cortical brain lesions. *Neurosci Lett* **355**, 93–96.

Calautti C & Baron JC (2003). Functional neuroimaging studies of motor recovery after stroke in adults: a review. *Stroke* **34**, 1553–1566.

Calautti C, Leroy F, Guincestre JY *et al*. (2003). Displacement of primary sensorimotor cortex activation after subcortical stroke: a longitudinal PET study with clinical correlation. *Neuroimage* **19**, 1650–1654.

Cao J, Murata N, Amari S *et al.* (2000). Single-trial magnetoencephalographic data decomposition and localization based on independent component analysis approach. *IEICE Transactions Fundamentals Electronics, Comms Computer Sci* **9**, 1757–1766.

Cichocki A & Amari SI (2002). *Adaptive Blind Signal and Image Processing*. John Wiley & Sons, Chichester, UK.

Cicinelli P, Marconi B, Zaccagnini M *et al*. (2006). Imagery-induced cortical excitability changes in stroke: a transcranial magnetic stimulation study. *Cereb Cortex* **16**, 247–253.

Conway BA, Halliday DM, Farmer SF *et al*. (1995). Synchronization between motor cortex and spinal motoneuronal pool during the performance of a maintained motor task in man. *J Physiol* **489**, 917–924.

Craelius W (2002). The bionic man: restoring mobility. *Science* **295**, 1018–1021.

Croft RJ & Barry RJ (2000). Removal of ocular artifact from the EEG: a review. *Neurophysiol Clin* **30**, 5–19.

Culpepper BJ & Keller RM (2003). Enabling computer decisions based on EEG input. *IEEE Trans Neural Syst Rehabil Eng* **11**, 354–360.

Del Gratta C, Pizzella V, Tecchio F & Romani G-L (2001). Magnetoencephalography – a non invasive brain imaging method with 1 ms time resolution. *Rep Prog Phys* **64**, 1759–1814.

Delorme A & Makeig S (2004). EEGLAB: an open source toolbox for analysis of single-trial EEG dynamics including independent component analysis. *J Neurosci Meth* **134**, 9–21.

Flor H, Nikolajsen L & Staehelin Jensen T (2006). Phantom limb pain: a case of maladaptive CNS plasticity? *Nat Rev Neurosci* **7**, 873–881.

Fridman EA, Hanakawa T, Chung M, Hummel F, Leiguarda RC & Cohen LG (2004). Reorganization of human premotor cortex after stroke recovery. *Brain* **127**, 747–758.

Gastaut H (1952). Etude electrocorticographique de la reactivite des rythmes rolandiques. *Rev Neurol* **87**, 176–182.

Gerloff C, Braun C, Staudt M *et al*. (2006*a*). Coherent corticomuscular oscillations originate from primary motor cortex: evidence from patients with early brain lesions. *Hum Brain Mapp* **27**, 789–798.

Gerloff C, Bushara K, Sailer A *et al*. (2006*b*). Multimodal imaging of brain reorganization in motor areas of the contralesional hemisphere of well recovered patients after capsular stroke. *Brain* **129**, 791–808.

Goncharova II, McFarland DJ, Vaughan TM *et al*. (2003). EMG contamination of EEG: spectral and topographical characteristics. *Clin Neurophysiol* **114**, 1580–1593.

Gordon J, Ghilardi MF & Ghez C (1995). Impairments of reaching movements in patients without proprioception. *J Neurophysiol* **73**, 347–360.

Graimann B, Townsend G & Pfurtscheller G (2006). Brain-computer communication – A brief introduction (Technical Report). BCI-Info, BCI Laboratory, Technische Universität Graz, Graz, Austria.

Gross J, Tass PA, Salenius S *et al*. (2000). Cortico-muscular synchronization during isometric muscle contraction in humans as revealed by magnetoencephalography. *J Physiol* **527**, 623–631.

Hallet M (1996). Transcranial magnetic stimulation: a tool for mapping the central nervous system. *Electroencephalogr Clin Neurophysiol Suppl* **46**, 43–51.

Hämäläinen MS & Ilmoniemi RJ (1994). Interpreting magnetic fields of the brain: minimum norm estimates. *Med Biol Eng Comput* **32**, 35–42.

Hari R & Kaukoranta E (1985). Neuromagnetic studies of somatosensory system: principles and examples. *Prog Neurobiol* **24**, 233–256.

Hari R, Reinikainen K, Kaukoranta E *et al*. (1984). Somatosensory evoked magnetic fields from SI and SII in man. *Electroencephalogr Clin Neurophyisol* **57**, 254–263.

Heeger DJ, Huk AC, Geisler WS *et al*. (2000). Spikes versus BOLD: what does neuroimaging tell us about neuronal activity? *Nat Neurosci* **3**, 631–633.

Heeger DJ & Ress D (2002). What does fMRI tell us about neuronal activity? *Nat Rev Neurosci* **3**, 142–151.

Heiss WD & Graf R (1994). The ischemic penumbra. *Curr Opin Neurol* **7**, 11–19.

Huang JC, Nicholson C, Okada Y & C (1990). Distortion of magnetic evoked fields and surface potentials by conductivity differences and boundaries in brain tissue. *Biophys J* **57**, 1155–1667.

Huang MX, Aine C, Davis L *et al*. (2000). Sources on the anterior and posterior banks of the central sulcus identified from magnetic somatosensory evoked responses using multistart spatio-temporal localization. *Hum Brain Mapp* **11**, 59–76.

Hummel FC & Cohen LG (2005). Drivers of brain plasticity. *Curr Opin Neurol* **18**, 667–674.

Hung CI, Lee PL, Wu YT *et al*. (2005). Recognition of motor imagery electroencephalography using independent component analysis and machine classifiers. *Ann Biomed Eng* **33**, 1053–1070.

Hyvärinen A, Karhunen J & Oja E (2001). *Independent Component Analysis*. John Wiley & Sons, Chichester, UK.

Johansen-Berg H, Rushworth MF, Bogdanovic MD *et al*. (2002). The role of ipsilateral premotor cortex in hand movement after stroke. *Proc Natl Acad Sci U S A* **99**, 14518–14523.

Johansson RS & Westling G (1987). Signals in tactile afferents from the fingers eliciting adaptive motor responses during precision grip. *Exp Brain Res* **66**, 141–154.

Kawamura T, Nakasato N, Seki K *et al*. (1996). Neuromagnetic evidence of pre and post-central cortical sources of somatosensory evoked responses. *Electroencephalogr Clin Neurophysiol* **100**, 44–50.

Keene DL, Whiting S & Ventureyra EC (2000). Electrocorticography. *Epileptic Disord* **2**, 57–63.

Kilner JM, Baker SN, Salenius S *et al*. (2000). Human cortical muscle coherence is directly related to specific motor parameters. *J Neurosci* **20**, 8838–8845.

Kotani K, Kinomoto Y, Yamada M *et al*. (2004). Spatiotemporal patterns of movement-related fields in stroke patients. *Neurol Clin Neurophysiol* **30**, 2004–2063.

Kristeva R, Popa T, Chakarov V *et al*. (2004). Cortico-muscular coupling in a patient with postural myoclonus. *Neurosci Lett* **366**, 259–263.

Kristeva-Feige R, Fritsch C, Timmer J *et al*. (2002). Effects of attention and precision of exerted force on beta range EEG-EMG synchronization during a maintained motor contraction task. *Clin Neurophysiol* **113**, 124–131.

Kristeva-Feige R, Rossi S, Pizzella V *et al*. (1996). Changes in movement-related brain activity during transient deafferentation: a neuromagnetic study. *Brain Res* **714**, 201–208.

Lauer R, Peckham P, Kilgore K *et al*. (2000*a*). Applications of cortical signals to neuroprosthetic control: a critical review. *IEEE Trans Rehabil Eng* **8**, 205–208.

Lauer RT, Peckham PH, Kilgore KL *et al*. (2000*b*). Applications of cortical signals to neuroprosthetic control: a critical review. *IEEE Trans Rehabil Eng* **8**, 205–208.

Lee PL, Hsieh JC, Wu CH *et al*. (2006). The brain computer interface using flash visual evoked potential and independent component analysis. *Ann Biomed Eng* **34**, 1641–1654.

Lotze M & Cohen LG (2006). Volition and imagery in neurorehabilitation. *Cogn Behav Neurol* **19**, 135–140.

Loubinoux I, Carel C, Pariente J *et al*. (2003). Correlation between cerebral reorganization and motor recovery after subcortical infarcts. *Neuroimage* **20**, 2166–2180.

McFarland D, Lefkowicz A & Wolpaw J (1997). Design and operation of an EEG-based brain–computer interface with digital signal processing technology. *Behav Res Meth Instrum Comput* **29**, 337–345.

Maclin EL, Rose DF, Knight JE *et al*. (1994). Somatosensory evoked magnetic fields in patients with stroke. *Electroencephalogr Clin Neurophysiol* **91**, 468–475.

Makeig S, Bell AJ, Jung TP *et al*. (1996). Independent component analysis of electroencephalographic data. In *Advances in Neural Information Processing Systems*, Vol. 8, pp. 145–151, ed. Jordan MI, Kearns MJ & Solla SA. MIT Press, Cambridge, MA.

Makeig S, Debener S, Onton J *et al*. (2004). Mining event-related brain dynamics. *Trends Cogn Sci* **8**, 204–210.

Makeig S, Enghoff S, Jung TP *et al*. (2000). Natural basis for efficient brain-actuated control. *IEEE Trans Rehabil Eng* **8**, 208–211.

Makeig S, Westerfield M, Jung TP *et al*. (2002). Dynamic brain sources of visual evoked responses. *Science* **295**, 690–694.

Maynard EM, Nordhausen CT & Normann RA (1997). The Utah intracortical electrode array: a recording structure for potential brain–computer interfaces. *Electroencephalogr Clin Neurophysiol* **102**, 228–239.

Moore MM (2003). Real-world applications for brain–computer interface technology. *IEEE Trans Neural Syst Rehabil Eng* **11**, 162–165.

Mosher JC & Leahy RM (1999). Source localization using recursively applied and projected (RAP) MUSIC. *IEEE Trans Sig Proc* **47**, 332–345.

Mosher JC, Lewis PS & Leahy RM (1992). Multiple dipole modeling and localization from spatiotemporal MEG data. *IEEE Trans Biomed Eng* **39**, 541–557.

Murthy VN & Fetz EE (1992). Coherent 25- to 35-Hz oscillations in the sensorimotor cortex of awake behaving monkeys. *Proc Natl Acad Sci U S A* **89**, 5670–5674.

Navarro X, Krueger T, Lago N *et al*. (2005). A critical review of interfaces with the peripheral nervous system for the control of neuroprostheses and hybrid bionic systems. *J Pher Nerv Sys* **10**, 229–258.

Nicolelis MA, Lin RC, Woodward DJ *et al*. (1993). Induction of immediate spatiotemporal changes in thalamic networks by peripheral block of ascending cutaneous information. *Nature* **361**, 533–536.

Niedermeyer E & Lopes da Silva F (1997). *Electroencephalography: Basic Principles, Clinical Applications, and Related Fields*. Williams & Wilkins, Baltimore, MD.

Oliviero A, Tecchio F, Zappasodi F *et al*. (2004). Brain sensorimotor hand area functionality in acute stroke: insights from magnetoencephalography. *Neuroimage* **23**, 542–550.

Pascual-Marqui RD, Michel CM & Lehman D (1995). Low resolution electromagnetic tomography: a new method for localising electrical activity in the brain. *Int J Psychophysiol* **18**, 49–65.

Piccione F, Giorgi F, Tonin P *et al*. (2006). P300-based brain computer interface: reliability and performance in healthy and paralysed participants. *Clin Neurophysiol* **117**, 531–537.

Pineiro R, Pendlebury S, Johansen-Berg H *et al*. (2001). Functional MRI detects posterior shifts in primary sensorimotor cortex activation after stroke: evidence of local adaptive reorganization? *Stroke* **32**, 1134–1139.

Piper HE (1907). Uber den willkurlichen Muskeltetanus. *Pflugers Gesamte Physiologie Des Menschen Tiere* **119**, 301–338.

Piper HE (1912). *Elektrophysiologie Menschlicher Muskeln*. Springer, Berlin.

Pizzella V, Tecchio F, Romani GL *et al*. (1999). Functional localization of the sensory hand area with respect to the motor central gyrus knob. *Neuroreport* **10**, 3809–3814.

Popovic D & Sinkjaer T (2000). *Control of Movement for the Physically Disabled*. Springer-Verlag.

Popovic M (2003). Control of neural prostheses for grasping and reaching. *Med Engineering Physics* **25**, 41–50.

Porcaro C, Barbati G, Zappasodi F *et al*. (2007). Hand sensory-motor cortical network assessed by functional source separation. *Hum Brain Mapp* in press.

Porcaro C, Zappasodi F, Barbati G *et al*. (2006). Fetal auditory responses to external sounds and mother's heart beat: detection improved by independent component analysis. *Brain Res* **26**, 51–58.

Prochazka A, Gauthier M, Wieler M *et al*. (1997). The bionic glove: An electrical stimulator garment that provides controlled grasp and hand opening in quadriplegia. *Arch Phys Med Rehabilitation* **78**, 1–7.

Puce A, Constable RT, Luby ML *et al*. (1995). Functional magnetic resonance imaging of the sensory and motor cortex: comparison with electrophysiological localization. *J Neurosurg* **83**, 262–270.

Qin L, Ding L & He B (2004). Motor imagery classification by means of source analysis for brain–computer interface applications. *J Neural Eng* **1**, 135–141.

Rees G, Friston K & Koch C (2000). A direct quantitative relationship between the functional properties of human and macaque V5. *Nat Neurosci* **3**, 716–723.

Rossi S, Pasqualetti P, Tecchio F *et al*. (1998*a*). Corticospinal excitability modulation during mental simulation of wrist movements in human subjects. *Neurosci Lett* **243**, 147–151.

Rossi S, Pasqualetti P, Tecchio F *et al*. (1998*b*). Modulation of corticospinal output to human hand muscles following deprivation of sensory feedback. *Neuroimage* **8**, 163–175.

Rossini PM, Calautti C, Pauri F *et al*. (2003). Post-stroke plastic reorganisation in the adult brain. *Lancet Neurol* **2**, 493–502.

Rossini PM, Caltagirone C, Castriota-Scanderbeg A *et al*. (1998). Hand motor cortical area reorganization in stroke: a study with fMRI, MEG and TCS maps. *Neuroreport* **9**, 2141–2146.

Rossini PM, Martino G, Narici L *et al*. (1994*a*). Short-term brain 'plasticity' in humans: transient finger representation changes in sensory cortex somatotopy following ischemic anaesthesia. *Brain Res* **642**, 169–177.

Rossini PM, Narici L, Martino G *et al*. (1994*b*). Analysis of interhemispheric asymmetries of somatosensory evoked magnetic fields to right and left median nerve stimulation. *Electroencephalogr Clin Neurophysiol* **91**, 476–482.

Rossini PM, Rossi S, Pasqualetti P *et al*. (1999). Corticospinal excitability modulation to hand muscles during movement imagery. *Cerebral Cortex* **9**, 161–167.

Rossini PM, Rossi S, Tecchio F *et al*. (1996*a*). Focal brain stimulation in healthy humans: motor maps changes following partial hand sensory deprivation. *Neurosci Lett* **214**, 191–195.

Rossini PM, Tecchio F, Pizzella V *et al*. (2001). Interhemispheric differences of sensory hand areas after monohemispheric stroke: MEG/MRI integrative study. *Neuroimage* **14**, 474–485.

Rossini PM, Tecchio F, Sabato A *et al*. (1996*b*). The role of cutaneous inputs during magnetic transcranial stimulation. *Muscle Nerve* **19**, 1302–1309.

Sadato N, Zeffiro TA, Campbell G *et al*. (1995). Regional cerebral blood flow changes in motor cortical areas after transient anesthesia of the forearm. *Ann Neurol* **37**, 74–81.

Sainburg RL, Poizner H & Ghez C (1998). Loss of proprioception produces deficits in interjoint coordination. *J Neurophysiol* **82**, 1–15.

Schaechter JD (2004). Motor rehabilitation and brain plasticity after hemiparetic stroke. *Prog Neurobiol* **73**, 61–72.

Scherg M & Berg P (1991). Use of prior knowledge in brain electromagnetic source analysis. *Brain Topogr* **4**, 143–150.

Scott SH (2004). Optimal feedback control and the neural basis of volitional motor control. *Nat Rev Neurosci* **5**, 532–546.

Serby H, Yom-Tov E & Inbar GF (2005). An improved P300-based brain–computer interface. *IEEE Trans Neural Syst Rehabil Eng* **13**, 89–98.

Sharma N, Pomeroy VM & Baron JC (2006). Motor imagery: a backdoor to the motor system after stroke? *Stroke* **37**, 1941–1952.

Stein R, Peckham P & Popovic D (1992). *Neural Prosthesis*. Oxford University Press, Oxford, UK.

Tang AC, Sutherland MT & McKinney CJ (2005). Validation of SOBI components from high-density EEG. *Neuroimage* **25**, 539–553.

Tecchio F, Bicciolo G, De Campora E *et al*. (2000*a*). Tonotopic cortical changes following stapes substitution in otosclerotic patients: a magnetoencephalographic study. *Hum Brain Mapp* **10**, 28–38.

Tecchio F, Graziadio S, Barbati G *et al*. (2007*a*). Dynamic gamma-band synchrony: a neural code of sensorimotor dexterity. *Neuroimage*, **35**, 185–193.

Tecchio F, Padua L, Aprile I *et al*. (2002). Carpal tunnel syndrome modifies sensory hand cortical somatotopy: a MEG study. *Hum Brain Mapp* **17**, 28–36.

Tecchio F, Pasqualetti P, Pizzella V *et al*. (2000*b*). Morphology of somatosensory evoked fields: inter-hemispheric similarity as a parameter for physiological and pathological neural connectivity. *Neurosci Lett* **287**, 203–206.

Tecchio F, Pasqualetti P, Zappasodi F *et al*. (2007*b*). Prognostic value of magnetoencephalography parameteres in acute monohemispheric stroke. *J Neurol*, **35**, 185–193.

Tecchio F, Porcaro C, Zappasodi F *et al*. (2006*a*). Cortical short-term fatigue effects assessed via rhythmic brain-muscle coherence. *Exp Brain Res* **174**, 144–151.

Tecchio F, Rossini PM, Pizzella V *et al*. (1997). Spatial properties and interhemispheric differences of the sensory hand cortical representation: a neuromagnetic study. *Brain Res* **767**, 100–108.

Tecchio F, Zappasodi F, Melgari JM *et al*. (2006*b*). Sensory–motor interaction in primary hand cortical areas: a MEG assessment. *Neuroscience* **141**, 533–542.

Tecchio F, Zappasodi F, Pasqualetti P *et al*. (2005*a*). Rhythmic brain activity at rest from rolandic areas in acute mono-hemispheric stroke: a magnetoencephalographic study. *Neuroimage* **28**, 72–83.

Tecchio F, Zappasodi F, Pasqualetti P *et al*. (2005*b*). Neural connectivity in hand sensorimotor brain areas: an evaluation by evoked field morphology. *Hum Brain Mapp* **24**, 99–108.

Tecchio F, Zappasodi F, Pasqualetti P *et al*. (2006*c*). Long-term effects of stroke on neuronal rest activity in rolandic cortical areas. *J Neurosci Res* **83**, 1077–1087.

Tecchio F, Zappasodi F, Tombini M *et al*. (2006*d*). Brain plasticity in recovery from stroke: an MEG assessment. *Neuroimage* **32**, 1326–1334.

Terao Y, Ugawa Y, Hanajima R *et al*. (1999). Air-puff-induced facilitation of motor cortical excitability studied in patients with discrete brain lesions. *Brain* **122**, 2259–2277.

Thickbroom GW, Byrnes ML, Archer SA *et al*. (2004). Motor outcome after subcortical stroke correlates with the degree of cortical reorganization. *Clin Neurophysiol* **115**, 2144–2150.

Timmermann L, Gross J, Dirks M *et al*. (2003). The cerebral oscillatory network of parkinsonian resting tremor. *Brain* **126**, 199–212.

Treisman AM & Kanwisher NG (1998). Perceiving visually presented objects: Recognition, awareness, and modularity. *Current Opinion Neurobiol* **8**, 218–226.

Vigario R, Jousmaki V, Hamalainen M *et al*. (eds) (1997). Independent component analysis for identification of artifacts in magnetoencephalographic recordings. In *Advances in Neural Information Processing Systems*, pp. 229–235. MIT Press, Cambridge.

Volkmann J, Joliot M, Mogilner A *et al*. (1996). Central motor loop oscillations in parkinsonian resting tremor revealed by magnetoencephalography. *Neurology* **46**, 1359–1370.

Vrba J & Robinson SE (2001). Signal processing in magnetoencephalography. *Methods* **25**, 249–271.

Wikstrom H, Huttunen J, Korvenoja A *et al*. (1996). Effects of interstimulus interval on somatosensory evoked magnetic fields (SEFs): a hypothesis concerning SEF generation at the primary sensorimotor cortex. *Electroencephalogr Clin Neurophysiol* **100**, 479–487.

Wikstrom H, Roine RO, Salonen O *et al*. (1997). Somatosensory evoked magnetic fields to median nerve stimulation: interhemispheric differences in a normal population. *Electroencephalogr Clin Neurophysiol* **104**, 480–487.

Wolpaw JR, Birbaumer N, McFarland DJ *et al*. (2002). Brain–computer interfaces for communication and control. *Clin Neurophysiol* **113**, 767–791.

Xu N, Gao X, Hong B *et al*. (2004). BCI Competition 2003 – Data set IIb: enhancing P300 wave detection using ICA-based subspace projections for BCI applications. *IEEE Trans Biomed Eng* **51**, 1067–1072.

Zappasodi F, Pasqualetti P, Ercolani M *et al*. (2006). Hand cortical representation at rest and during activation: gender and age effects in the two hemispheres. *Clin Neurophysiol* **117**, 1518–1528.

Ziehe A, Nolte G, Sander T *et al*. (2000). Artifact reduction in magnetoneurography based on time-delayed second-order correlations. *IEEE Trans Biomed Eng* **47**, 75–87.

Ziehe A, Nolte G, Sander T *et al*. (2001). A comparison of ICA-based artifact reduction methods for MEG. In *Proceedings of the 12th International Conference on Biomagnetism*, pp. 895–898. Helsinki University of Technolology, Espoo, Finland.

Acknowledgements

This work was partially supported by the RBNE01AZ92, PRIN 2005027850 and PRIN 2005063547 of the Italian Department of University and Research (MIUR) and by the European IST/FET Integrated Project NEUROBOTICS – the fusion of NEUROscience and roBOTICS, Project no. 001917 under the 6th Framework Programme.